Proceedings of the Institute of Acoustics

FOLDED SHELL PROJECTOR

C.J. Purcell and Y.R. Bonin

Defence Research Establishment Atlantic, Dartmouth, N.S. Canada, B2Y 3Z7

1 Introduction

Defence Research Establishment Atlantic (DREA) has recently disclosed a design for a flextensional transducer called the Folded Shell Projector (FSP) [1]. The FSP is a compact, low-frequency underwater sound source which has potential applications in low frequency sonar systems.

The FSP can be described as a variation on the barrel stave projector (BSP). The BSP achieves the required values for stiffness and mechanical transformer ratio for its radiating surface by having slots in a solid axisymmetric shell [2] or individual staves separated by slots [3]. The slots must be waterproofed by a polymer membrane (e.g. neoprene) called the "boot". Under hydrostatic loading the boot is pushed into the slots leading to depth dependence of the resonance frequency and source level. Thus for some applications, the BSP may require a gas pressure compensation system to be fitted [4], with its attendant cost and complexity.

There have been previous efforts at DREA to build bootless variants of the BSP [5], and the FSP is the most recent attempt. The FSP design uses folds instead of slots and since the resultant one-piece shell is inherently waterproof, the boot is not required (although some FSP applications may still need a corrosion proof coating). The basic concept of the folded shell projector is illustrated in Figure 1.

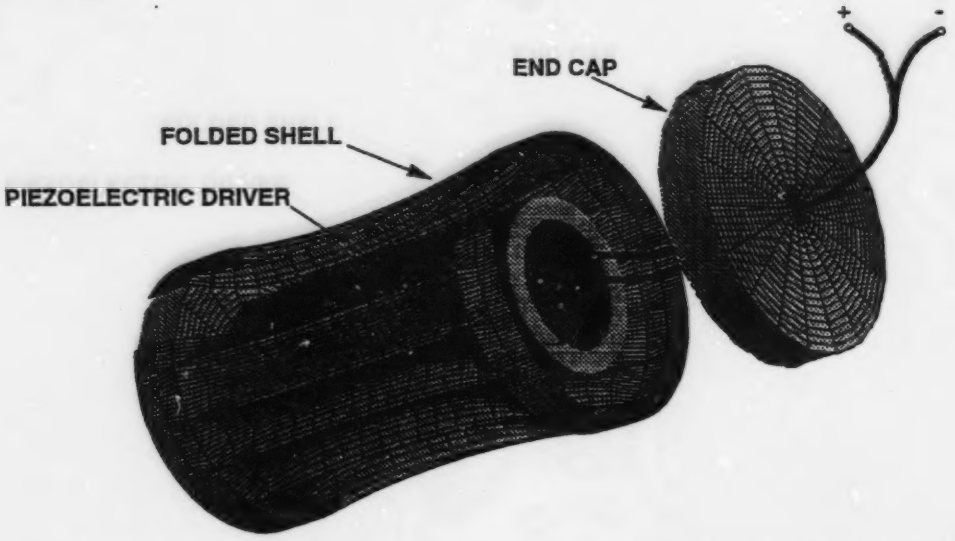

Figure 1: Simplified view of folded shell projector, with one fold cut away and end cap removed.

2 Design and Construction Methods

A combination of static finite element analysis (using MAVART3D) and equivalent circuit analysis based on [6] was used to design the prototype FSP.

The equivalent circuit analysis identified the shell's static radial to axial mechanical transformer ratio and the axial shell compliance as key design parameters. In this report, the shell transformer ratio is taken to be the ratio of the mean radial deflection of points in the middle of the folds to the mean axial deflection of points on one of the shell ends, under a static axial load.

This preliminary work provided shell transformer ratio and compliance goals sufficent to guide construction of a MAVART3D finite element model of an axisymmetric shell with small superimposed corrugations. Initial attempts indicated that sinusoidal corrugations would not be compliant enough in the tangential direction, and attention was focused on surfaces for which the exterior portion of the corrugation ended in a sharp fold. The shape of the folds were taken initially to be parabolas along both tangential and axial directions. As the modelling progressed it became apparent that higher order polynomials (4th) were required along the axial direction. The preliminary work assumed aluminum alloy as the shell material and established that wall thicknesses in the 1 to 2 mm range were likely.

Given these wall thicknesses, and the complex shape, electroforming was selected as the most economical prototyping method. The range of electroformable metals (Cr, Au, Ag, Cu, Ni) is limited and of these Ni was the best choice. With this material choice, the folded shell dimensions were iterated until the MAVART3D results approached the target compliance and shell transformer ratio well enough to justify building a prototype. Because of the rather indirect modelling procedures used (finite element method combined with equivalent circuit analysis), it did not make sense to expend a lot of effort optimizing the shell to conform to somewhat uncertain targets. The goal was to come up with a design good enough to demonstrate proof of concept.

After the shell parameters described in Section 3 were frozen, a numerically controlled (NC) mill was programmed to make the electroforming mandrel. The electroforming process produces a perfect replica of the inside surface, but an irregular outside surface which needs to be machined to the outside contour of the shell. At this stage it was decided to deviate slightly from the final finite element model, in that the outer sharp cusps seen in Fig 1 were radiused. One quarter of the cross section at the mid plane of the modified shell is shown in Fig 2. The shape change associated with adding the radius slightly increased the mass and axial stiffness.

After the outside contours were milled the bulk of the Al mandrel was dissolved away in hot NaOH leaving the Ni shell unaffected. Mechanical measurements and vibration analysis on the shell were completed, and the prototype FSP was assembled using standard transducer construction techniques, with a piezoelectric driver consisting of a fiberglass wrapped stack of 10 parallel connected axially poled Navy Type III rings (50.8 mm o.d. by 38.1 mm i.d. by 10.1 mm thickness), two mild steel endcaps, two aluminum wiring covers, four stainless steel stress rods, a cast epoxy gland to waterproof the entry point for the electrical leads, and fittings for the future addition of a pressure compensation system. A photograph of the assembled projector is shown in Fig 3.

FOLDED SHELL PROJECTOR

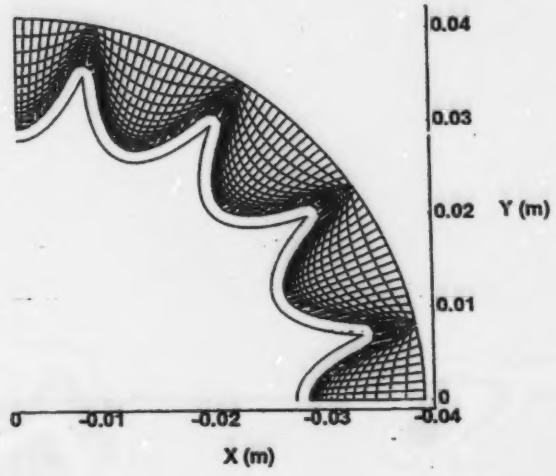

Figure 2: As-built folded shell design, showing radiused outer cusps. View from mid plane of 1/4 of the circumference.

3 Modelling the Shell

The starting point for the mathematical description of the folded shell was the equation for a conic space curve straddling the x axis and lying in the x-y plane. The angular extent of the conic as seen from the origin is $2\theta_0$ and r_0 is the radial distance of the conic endpoints from the origin.

By adding to the conic the difference between a circular arc of radius r_0 centered on the origin and joining the conic end points, and a straight line joining the end points, and extruding the result along the z axis, a surface shaped like a fold results. By making r_0 a function of z the radial location of the fold minima can be varied with height. In particular we chose:

$$r_0 = r_1 + \sqrt{R^2 - z_0^2} - \sqrt{R^2 - z^2} \tag{1}$$

where r_1 is the inner radius at height z_0 of a surface of revolution whose radius of curvature is R, upon which the fold has been placed. With the axial dependence of the depth of the fold given by $(\frac{z}{z_0})^4$ and taking the conic to be a parabola parametrized by s, with $0 < s < 1$, the surface of a single fold is given by:

$$\vec{X}[s,z] = \left\{ \begin{array}{l} r_0 \cos(\theta_0(2s-1)) + 4a_0(s^2-s)(1-(\frac{z}{z_0})^4), \\ r_0 \sin(\theta_0(2s-1)), \\ z \end{array} \right\} \tag{2}$$

If the depth parameter $a_0 = 0$ a surface of revolution that describes the outside of one stave of the barrel stave projector results. By varying the parameter a_0 we can superimpose folds of any depth on this surface. To construct a complete surface with n superimposed folds, the angle θ_0 was chosen to be π/n and the surface given by Equation 2 was sequentially rotated by $2\theta_0$ about the z axis n times. The annular flanges of radius r_1 added to the top and bottom of the folded portion of the surface (which are visible in Figure 3) are used to attach the end caps of the projector.

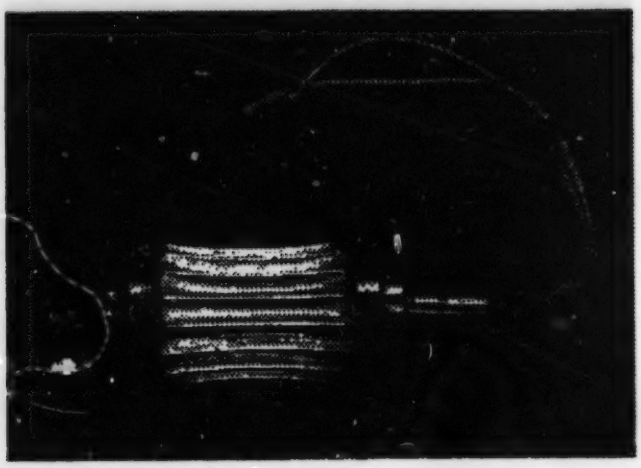

Figure 3: Photograph of assembled prototype folded shell projector.

The finite element model of the shell was built by coding Equation 2 in PATRAN Command Language (PCL) [7]. To create the outer surface of the shell, the outward normals to the inside surface (given by Equation 2) were calculated, and points on the outside surface were defined as laying a distance w along the outward pointing normals from the corresponding points on the inner surface. At the cusps of the folds, the normal is discontinuous, so at these points the normal was defined to be that corresponding to Equation 2 but with $a_0 = 0$. To minimize the required computer resources only 1/8 of the complete shell was modelled. The model used 2341 nodes and 384 hexahedral 20-noded elements, with two elements used through the wall thickness. Boundary conditions were applied to establish the required fixities and an axial loading of $1N$ was applied to all nodes on the inside surface of the flange. The fixities and loading simulated the conditions that would occur during use of the shell in a projector. After MAVART3D analysis the results were postprocessed to yield compliance and transformer ratio by averaging loads, and radial and axial deflections.

Since the model was described parametrically, it was easy to build and analyze dozens of variations on the shell design using the MAVART3D estimated values of transformer ratio and axial compliance to guide the search. The radius $r1$, height $z0$ and flange height were fixed by the constraints that the shell should have the same external dimensions as a 1200 Hz BSP. The final iterations involved just a_0, R and wall thickness w. Iterations were terminated when the target transformer ratio of 2:1 was reached, leaving the compliance less than the original goal. This was considered acceptable, since it was anticipated that the compliance would be increased in later designs when the shell material was changed from Ni to Al alloy.

Figure 4 shows the model with axial to radial transformer action corresponding to Table 1, which lists the MAVART3D predictions and shell parameters that were chosen for the prototype.

FOLDED SHELL PROJECTOR

Table 1: Final model parameters as selected for the prototype and as built.

Geometrical Parameters	Design Value	As Built
n (# of folds)	16	16
r1 (radius of flange)	39.9 mm	40.1± .2 mm
z0 (1/2 fold height)	51.1 mm	51.7± .2 mm
R (outer radius of curvature)	.30 m	
w (shell wall thickness)	1.25 mm	1.27 mm (+.05 mm -.13 mm)
a_0 (fold depth)	7.5 mm	
flange (height)	13.2 mm	12.7 ± .2 mm
Assumed Material Properties		
Ni Density	8904 kg/m^3	
Ni Young's Modulus	206.9 GPa	
Ni Poisson Ratio	.31	
Shell Properties		
Mass	395 g	435.2 g
Axial compliance	4.354×10^{-9} m/N	$6.2 \times 10^{-9} \pm 1.0 \times 10^{-9} m/N$
Radial/axial transformer ratio	2.268	1.0 ± .3

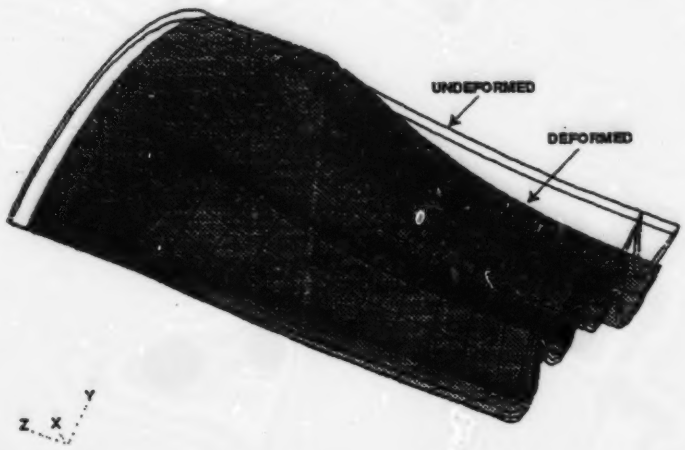

Figure 4: View of 1/8 folded shell model showing deformation and axial/radial transformer action.

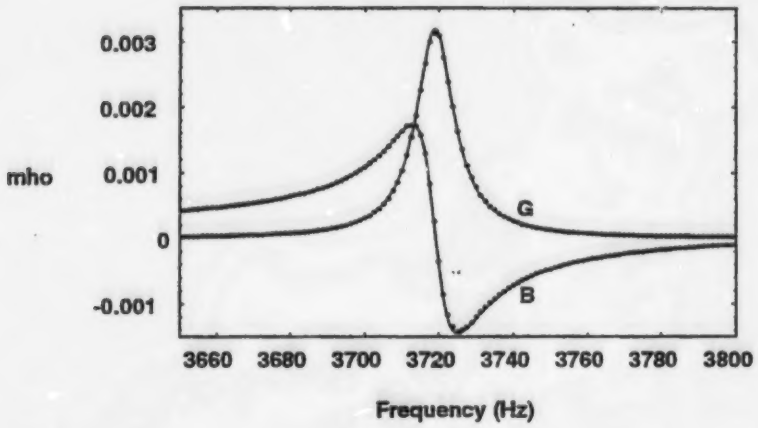

Figure 5: Conductance (G) and susceptance (B) vs frequency of the Folded Shell Projector in air. Dots are measured points, solid curve is equivalent circuit model fit to data.

4 Verification of Shell Parameters

After the shell was complete measurements were made to document the accuracy of the construction methods and to facilitate future modelling efforts, and are presented in Table 1.

Measurements of the shell axial compliance and transformer ratio were made by compressing the shell in a hydraulic press equipped with a force transducer to apply a known axial load, and using a dial indicator (sensitivity .01 mm) to measure deflections. Because the deflections are small, there was substantial scatter in the measurements however they indicate a significant disagreement between measured and model predictions for axial compliance and transformer ratio. This presumably reflects the mismatch between the finite element model and the prototype shell. It was previously noted that the prototype shell had 10% more mass than the finite element model prediction, and this mass gain was entirely in the vicinity of the cusp, where extra material thickness would have a substantial effect on compliance and transformer ratio.

5 Folded Shell Projector - Performance

Shallow water (30 m depth) calibrations of the prototype FSP were made at the DREA Acoustic Calibration Barge in Bedford Basin, Nova Scotia. The conductance and susceptance in air and in water, and the transmitting voltage response (TVR) are shown in Figures 5,6,7. The calibration results are summarized in Table 2.

The resonance frequency is higher than the design goal and reflects the fact that the FSP transformer ratio and the shell compliance are too low. Increasing both these parameters will be priorities for the next iteration of the design. The directivity was measured at resonance, in two planes, the x-y and x-z planes. The quoted efficiency was estimated using the directivity index (DI) measured in the x-z plane, neglecting the effect of the smaller x-y plane directivity. The efficiency is thus a lower bound. If the directivity had been integrated over all angles, the resulting efficiency could be

FOLDED SHELL PROJECTOR

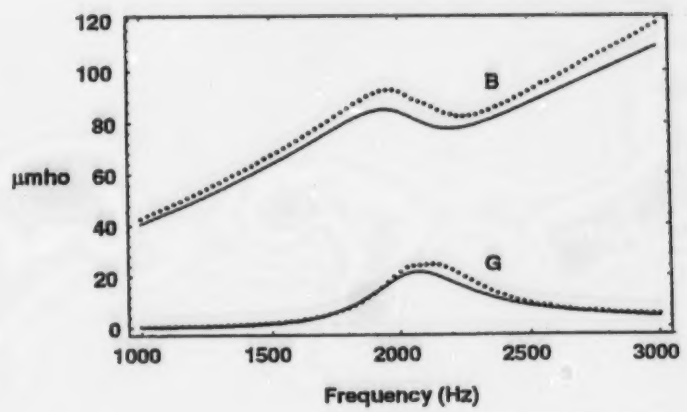

Figure 6: Conductance and susceptance vs frequency of the Folded Shell Projector at 30 m depth and driven with 3000 V. Dots are measured points, solid curve is equivalent circuit model fit to data.

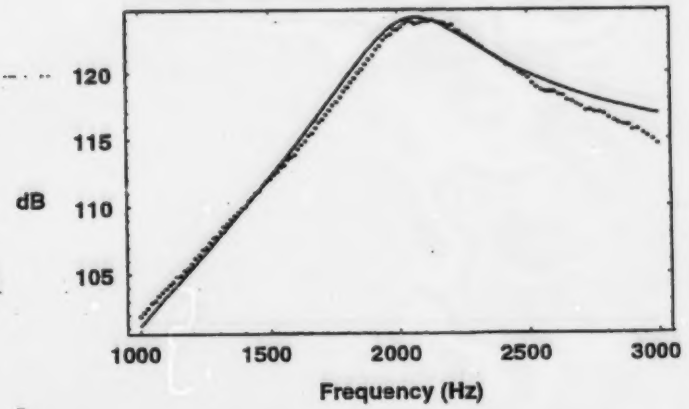

Figure 7: Transmitting voltage response in dB re 1 μPa/V @ 1 m for the Folded Shell Projector at 30 m depth and an applied drive voltage of 3000 V. Dots are measured points, solid curve is equivalent circuit model fit to data.

Table 2: Summary of Acoustic Performance of FSP @ 30 m depth and 3000 V (* at resonance).

Resonance frequency	2100 Hz
TVR*	123.8 dB re 1 μPa/V @ 1 m
SL* (@ 3 kV)	193.4 dB re 1 μPa @ 1 m
Bandwidth	530 Hz
Q	4.0
DI (@ 2100 Hz)	.98 dB
G*	24.5 μmho
B*	157.2 μmho
Efficiency	65. %
Mass	2.46 kg
Mass Figure of Merit	7.1 W/(kg-kHz-Q) @ 3000 V

several percent higher.

The mass Figure of Merit (FOM_m) [8] given in Table 2 is the ratio of radiated power to the product of mass, frequency and quality factor. To improve the FOM_m of the FSP, the density of the shell must be reduced and the shell design modified to lower the frequency.

Calibrations of the FSP were performed at drive levels ranging from 30-3000 V and the TVR was unaffected (to within measurement error) by drive level over this range.

Air backed flextensional projectors are inherently depth dependent. The depth dependence is evidenced mainly by a shift in resonance frequency. Measurements of the depth dependence of the FSP were made from the reseach vessel CFAV Endeavour in Exuma Sound. Admittance and TVR were measured for several depths between 50 m and 250 m. The measured resonance frequency shift is only 0.07 Hz/m, so for most applications the FSP would not require pressure compensation over this depth range.

6 Summary and Conclusions

There are several potential risk areas for this projector that can be identified at this stage and must be addressed in future research. The ultimate crush depth of the FSP is a concern, since the FSP lacks anything like the sudden rise in stiffness that the BSP benefits from, when the staves come into contact. Metal fatigue at the folds needs to be considered, since the sharp corners are stress raisers. The process used to make the folded shell described in this report would not lend itself to mass production. Manufacturing processes that could produce folded shells at low cost are being reviewed. The shell design should be adjusted to lower the frequency, and optimized for a high strength low density alloy, to reduce the weight.

A new design for a flextensional projector that uses a thin walled metal shell as the radiating surface has been described. The one-piece shell achieves low tangential stiffness by using folds so is inherently waterproof, and a rubber boot is not required. The prototype is insensitive to depth, has good bandwidth and efficiency.

Acknowledgements

Design, construction and testing of the prototype of the FSP involved contributions from many DREA staff members. Ron Fox, Gordon Chapman, Gary Fisher, David Lewis and Charles Reithmeier built the projector. Glenn Stewart performed calibrations at the DREA barge and Stuart Hutton assisted during the at-sea calibrations.

References

[1] C. J. Purcell. Folded Shell Projector. U.S. Patent No. 5,805,529, 8 Sept 1998.

[2] H.C. Merchant. Underwater Transducer Apparatus. U.S. Patent No. 3,258,738, 28 June 1966.

[3] G. W. McMahon and D. F. Jones. Barrel-Stave Projector. U.S. Patent No. 4,922,470, 1 May 1990.

[4] Y. R. Bonin and J. S. Hutton. Increasing the Depth Performance of Barrel Stave Projectors. *Canadian Acoustics*, 24(3):50, Sept 1996.

[5] D.F. Jones, N.N. Abboud, D.K. Vaughn, and G.L. Wojcik. Finite element analysis of a flextensional projector with a solid anisotropic composite shell. In *Proceedings of the Transducer Modelling Workshop*, pages 143–167, Naval Postgraduate School, Monterey, CA, July 1997.

[6] E.A. McLaughlin M.B. Moffett, J.F. Lindberg and J.M. Powers. An Equivalent Circuit Model for Barrel-Stave Flextensional Transducers. In *Third International Workshop on Transducers for Sonics and Ultrasonics*, pages 170–180, Orlando, FL, May 1992.

[7] MacNeal-Schwendler Corp, Los Angeles, California. *MSC/PATRAN*, 1998.

[8] D. F. Jones and J. F. Lindberg. Recent Transduction Developments in Canada and the United States. In *Proc I.O.A. Vol 17 Part 3*, pages 15–28, Birmingham, UK, 1995.